Optica Applicata, Vol. L, No. 4, 2020
DOI: 10.37190/oa200403

Efficient, low-cost optical coupling mechanism for TiO_2-SiO_2 sol-gel derived slab waveguide surface grating coupler sensors

Andrzej KAŹMIERCZAK[1*], Mateusz SŁOWIKOWSKI[1, 2], Krystian PAVŁOV[2], Maciej FILIPIAK[2], Michael VERVAEKE[3], Cuma TYSZKIEWICZ[4], Heidi OTTEVAERE[3], Ryszard PIRAMIDOWICZ[1], Paweł KARASIŃSKI[4]

[1]Institute of Microelectronics and Optoelectronics, Warsaw University of Technology, Koszykowa 75, 00-662 Warszawa, Poland

[2]CEZAMAT, Warsaw University of Technology, Poleczki 19, 02-822 Warsaw, Poland

[3]Vrije Universiteit Brussel, Department of Applied Physics and Photonics, Brussels Photonics (B-PHOT), Pleinlaan 2, 1050 Brussels, Belgium

[4]Department of Optoelectronics, Silesian University of Technology, Krzywoustego 2, 44−100 Gliwice, Poland

[*]Corresponding author: a.kazmierczak@imio.pw.edu.pl

We present an optical signal coupling scheme for slab waveguide surface grating coupler sensors. The proposed solution is based on the use of polymer microlenses. In this work we analyze two types of compact polymer lenses: the aspheric plano-convex lenses and Fresnel lenses. The feasibility of the proposed scheme is demonstrated by the experimental investigation into the optical signal coupling to the test structure of TiO_2-SiO_2 slab waveguide surface grating coupler using both types of lenses.

Keywords: polymer microlenses, optical coupling, surface grating couplers.

1. Introduction

Optical planar evanescent wave sensor structures have been studied intensively throughout the last decade by numerous researchers all over the world [1–4]. Among others, the solutions based on SOI (silicon on insulator) [5, 6], silicon nitride Si_3N_4 [7], tantalum pentoxide Ta_2O_5 [8], titania-silica TiO_2-SiO_2 [9–11] or polymer [12] waveguides have been reported. The vast majority of these sensors are based on integrated optical circuits and incorporate resonator-based sensors, *e.g.* ring resonators. Despite a profitable feature of high sensitivity, in most cases these sensors need full fabrication

process used for photonic integrated circuits and therefore suffer from complexity and expensiveness of fabrication technology.

In this paper we discuss the concept of an optical system containing polymer microlenses and surface grating coupler-based structures, produced in a sol-gel derived titania -silica film by a direct imprinting method constituting the starting point for the development of a low-cost multichannel label-free optical sensor system.

2. Structure concept

The use of planar surface grating couplers directly imprinted on sol-gel derived slab waveguides offers the possibility to reduce fabrication process complexity eventually leading to low-cost sensors [9–11]. The operation of such solutions is shown schematically in Fig. 1.

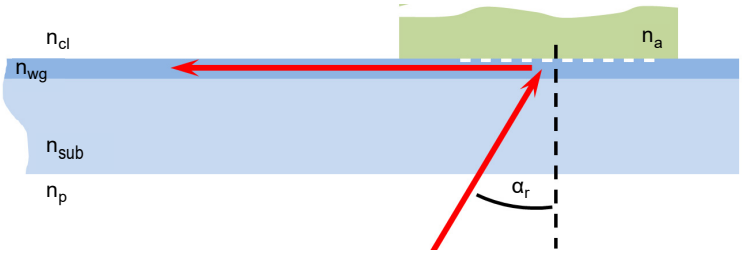

Fig. 1. Schematic representation of a surface grating coupler based biochemical sensor.

The sensor grating is imprinted in the waveguide layer (having refractive index n_{wg}) that is deposited on the substrate layer (n_{sub}, typically glass substrates are used). The waveguide layer is covered by the cladding layer (n_{cl}, typically the waveguide layer is exposed directly to surrounding atmosphere).

2.1. Grating coupler

When the lighting angle α_r of the grating structure fulfills the condition of the phase matching [9]:

$$\pm N = n_p \sin\alpha_r + r\frac{\lambda}{\Lambda} \tag{1}$$

then, the excitation of the mode of the effective refractive index N is taking place. The + or – sign has to be chosen depending whether the mode propagates along the $+x$ or $-x$ direction. In Eq. (1), $r = \pm 1, \pm 2, \pm 3\ldots$ stands for diffraction order, Λ is the grating period and n_p is the refractive index of the medium in which the angle α_r is measured. As one can see from Eq. (1), the resonance angle α_r is the function of the effective refractive index N that is affected by variation of the refractive index n_a of the medium above the grating. Therefore the ambient modification (*e.g.* change of the covering liquid composition or deposition of detected proteins) causes the variation of the reso-

nance angle α_r and can be detected by observing this variation. The operation of such sensor has been discussed in details in Refs. [10, 11].

The use of such sensors for a multichannel operation is not straightforward as in the case of slab waveguides, the optical signal is not confined in the horizontal direction and there is no possibility of using optical signal splitters [13] to split the signal among a number of resonator-based sensors. Consequently, when a slab waveguide surface grating coupler sensor is to be used for a parallel operation, one needs to insert a number of separated, quasi-parallel optical beams into the grating.

2.2. Multichannel optical coupling to surface grating sensor

The quasi-parallel beam can be obtained in the obvious way, when the end of the optical fiber illuminating a lens is placed at the focal point of this lens. When such operation is multiplied, *i.e.* a multitude of lenses is illuminated with the multitude of optical fibers, a number of optical quasi-parallel beams can be generated. This solution can be implemented by using a micro-lens array combined with an array of the optical fibers placed in a V-groove as schematically shown in Fig. 2.

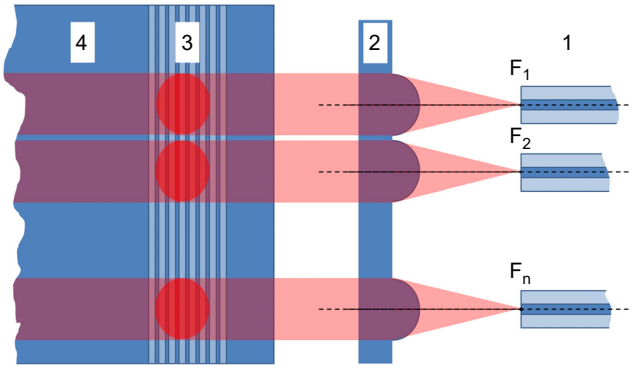

Fig. 2. Schematic representation of possible multichannel operation of a vertical grating coupler sensor. Light from an SMF array (1) illuminates an array of microlenses (2) forming a multitude of parallel beams that illuminate grating coupler (3) and form multiple guided modes in the slab waveguide (4).

A possibility of using polymer microlenses combined with standard optical single mode fibers (SMFs) for optical signal coupling to TiO_2-SiO_2 surface gratings is discussed in details in subsequent sections of this paper.

3. Micro-lens design and fabrication

Two different types of polymer microlenses were considered in the present study, namely plano-convex aspheric microlenses fabricated by hot embossing process and Fresnel microlenses fabricated by e-beam lithography on the glass substrate. Lenses fabricated in both processes shared the same geometry, *i.e.* radii of lenses were set to 250 μm and focal lengths ranged between 0.4 and 0.8 mm.

3.1. Aspheric lenses fabrication

The aspheric lenses were fabricated at B-Phot, Vrije Universiteit Brussel (VUB), Belgium, premises by hot embossing a brass mold (fabricated using a micro-diamond tooling machine 350FG from Moore Nanotech) on the PMMA substrate at temperature of 120°C (above the glass transition temperature but well below melt conditions) and with the force of 3 kN (using Jenoptik HEX04 hot embossing tool). Figure 3 shows the micrographs of the fabricated aspheric microlenses array.

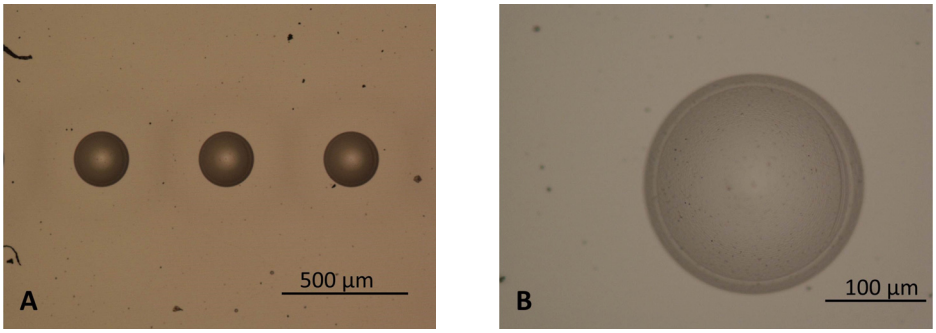

Fig. 3. Optical micrographs of aspheric microlenses fabricated at VUB by hot embossing process.

In Fig. 3**a** a part of a microlenses array is depicted. Proper shape and regular spacing between lenses can be noticed. In Fig. 3**b** a close up micrograph of the single lens is shown. A proper circular shape of the lens can be observed with only some minor imperfection on the right hand side of the lens boundary.

3.2. Fresnel lenses fabrication

The Fresnel lenses were fabricated at the Warsaw University of Technology (WUT), Poland, premises in CEZMAT laboratory by a direct electron beam writing on PMMA layer deposited on 700 µm glass substrate. The pattern was manufactured using grayscale lithography – a technique that creates three-dimensional features in a single exposure by modulating an electron dose in each spot or subregion. After polymer development, the desired three-dimensional structure is revealed. However, grayscale lithography has its limitations – electron resist films, thicker than 10 µm, may only be manufactured by multiple spin-coating, which negatively affects film uniformity. Moreover, surface roughness of the final structure increases with modulation depth, which in turn affects the optical performance. In order to achieve 250 µm diameter and desired focal length of 700 µm, a spherical Fresnel lens was designed and manufactured, as its height can be easily controlled.

The substrate was spin-coated with 10 µm layer of PMMA950 positive electron beam resist and 40 nm of AR-PC 5091 Electra conductive polymer. Fresnel lens pattern with 2 µm depth modulation was exposed using a JEOL JBX9300FS electron beam lithography tool. The conductive layer was removed in deionized water and the pattern

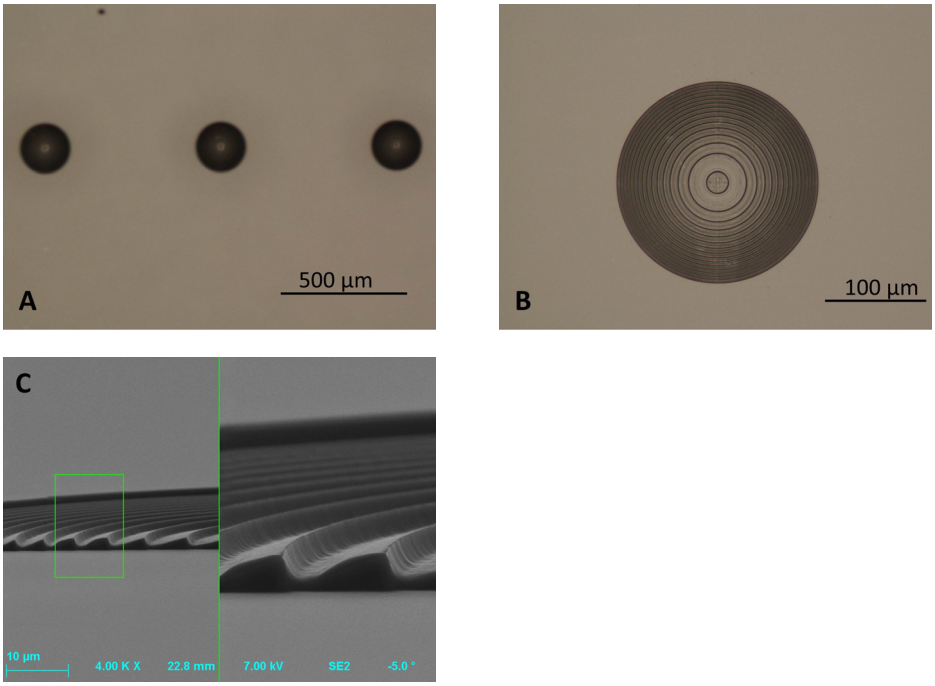

Fig. 4. Optical micrographs of Fresnel microlenses fabricated at WUT by electron-beam lithography (**a**, **b**) and the SEM micrograph of a fabricated Fresnel microlens profile (**c**).

was developed using 1:1 MIBK-IPA mixture. The lenses were then annealed in 115°C for 5 minutes to further decrease surface roughness. Figure 4 shows the micrographs of the fabricated Fresnel microlenses array.

In Fig. 4**a** a part of a microlenses array is depicted. Also in this case a proper shape and regular spacing between lenses can be noticed. In Fig. 4**b** a close up micrograph of the single Fresnel lens is shown. A correct circular shape of the Fresnel rings can be observed. Figure 4**c** shows the cross-section of the fabricated Fresnel microlens. It is noticeable that the maximum thickness of the PMMA layer is the same in each section, while some minor local deviations from the intended lens shape occur.

4. Assembling lenses with single mode fiber

In the first step of the analysis, the fabricated microlenses were assembled with a single mode optical fiber in order to verify the possibility of generating a quasi-parallel beam. For this purpose, a light from a red laser source was coupled to an SMF. The fiber was placed on a 3D translation stage (Thorlabs MDT630B/M) providing an alignment accuracy better than ±100 nm in each axis. Using this stage, the fiber end was placed at the focal point of the lenses and the obtained beam profiles were acquired at the distance of about 30 cm from the lens surface with Thorlabs BC106 VIS beam profiler. Obtained profiles are shown in Fig. 5.

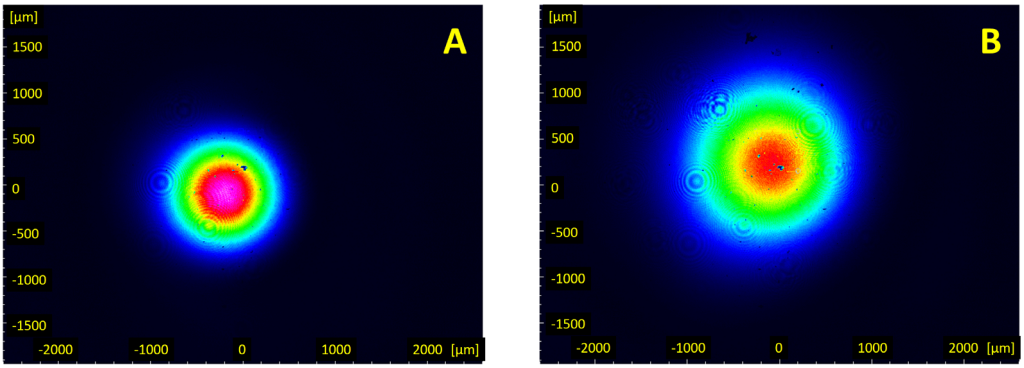

Fig. 5. Profiles of the optical beam after passing 30 cm distance generated with an SMF and PMMA lens: aspheric 250 µm diameter, 500 µm focal length lens (**a**), and Fresnel lens 250 µm diameter, 500 µm focal length (**b**).

It is noticeable in Fig. 5 that it was possible to obtain quasi-parallel beams with both types of lenses. Obviously, due to a small diameter of lenses, the obtained beams were not ideally parallel. In the case of an optical beam produced with an aspheric lens, the divergence angle can be estimated at approximately 0.2° while in the case of the beam produced with Fresnel lens, it can be estimated at 0.3°.

5. Optical signal coupling to the surface grating coupler

In order to asses microlenses usefulness for optical coupling to the surface grating coupler sensors, a test structure of TiO_2-SiO_2 slab waveguide with the embossed grating was used. The waveguide structure was fabricated at Silesian University of Technology, Poland, on a soda-lime microscope slide substrate by direct imprinting on a sol-gel derived TiO_2-SiO_2 waveguide layer. The exploited structure had following parameters:

- waveguide layer thickness d = 209 nm;
- waveguide layer refractive index n_{wg} = 1.79;
- grating amplitude h = 10 nm;
- groove density χ = 2400 g/mm;
- grating length 2 mm;
- grating width 10 mm.

The grating structure was tested using a goniometric setup and resonance coupling angles α_r were determined. The recorded modal spectra for both fundamental modes TE_0, TM_0 are shown in Fig. 6.

The optical coupling from the single mode fiber to the surface grating coupler was tested experimentally using the setup represented schematically in Fig. 7.

The single mode fiber (SMF) attached to the red light emitting laser source was placed on Thorlabs MDT630B/M 3D translation stage and its position was adjusted against the evaluated microlens in order to produce a quasi-parallel beam. The photonic chip con-

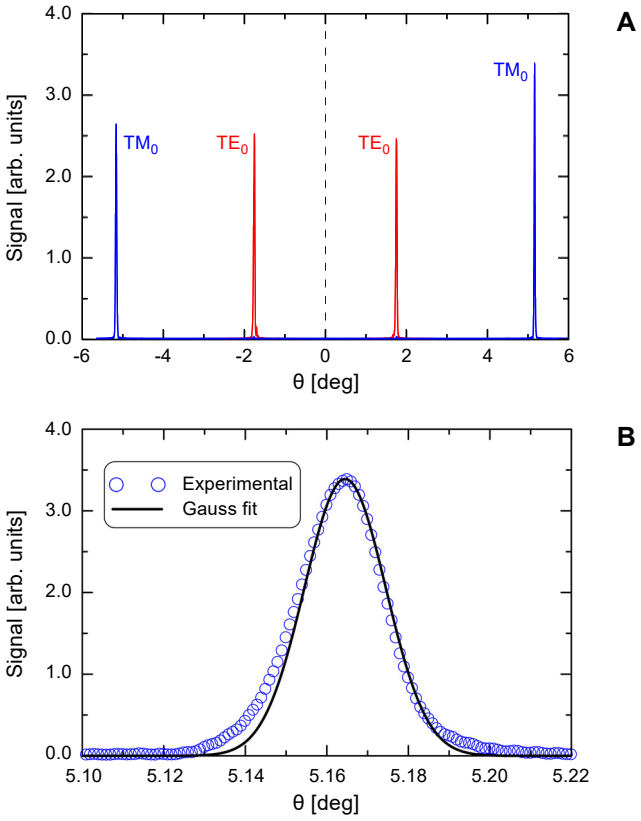

Fig. 6. Angle modal spectra of the surface grating coupler used in the experiment (**a**) and a close-up on the in-coupling peak TM_0 (FWHM = 0.024°) (**b**). The coupling angles are expressed as the angle between the normal and the input beam.

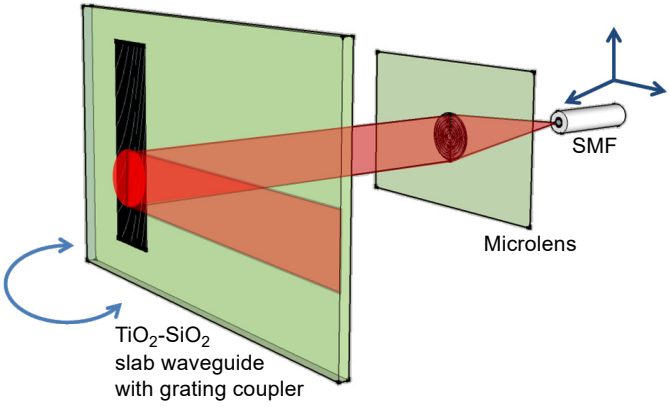

Fig. 7. Schematic representation of the experimental setup used for the observation of optical signal insertion to TiO_2-SiO_2 grating coupler with a microlens optical interface.

taining a vertical grating coupler was attached to the Thorlabs NR360S/M goniometric stage with a grating coupler located at the rotation axis of the stage. The stage was positioned in order to place the grating coupler in the quasi-parallel beam produced with the examined lens. The incidence angle of light was then adjusted with the goniometric stage in order to excite guided modes of the slab waveguide. The experiment is shown in Figs. 8 and 9 depicting the optical signal coupling to the surface grating coupler with a microlens interface. The optical signal from the SMF (3) is directed to the surface grating coupler (1) and in case of a resonance incidence angle, the output streak (2) is visible on the frosted part of the microscope slide substrate.

For both types of the used lenses, the optical coupling was easily achievable in the proximity of the optimal coupling angle for TM polarization (*i.e.* $\alpha_r \approx 5.165°$, Fig. 6).

The coupling efficiency was small, but this is an inherent feature of shallow and short period grating couplers. The longer period and deeper imprinted grating couplers should be used when one intends to increase the coupling efficiency, because this configuration of grating couplers leads to higher coupling tolerance and effectiveness. Such devices

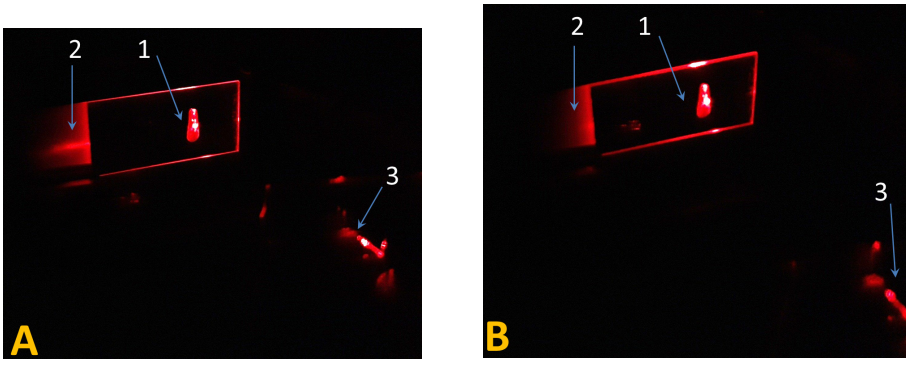

Fig. 8. The optical signal coupling to the grating coupler structure via PMMA aspheric microlens with an optimum incidence angle (**a**) and non-optimum incidence angle (**b**).

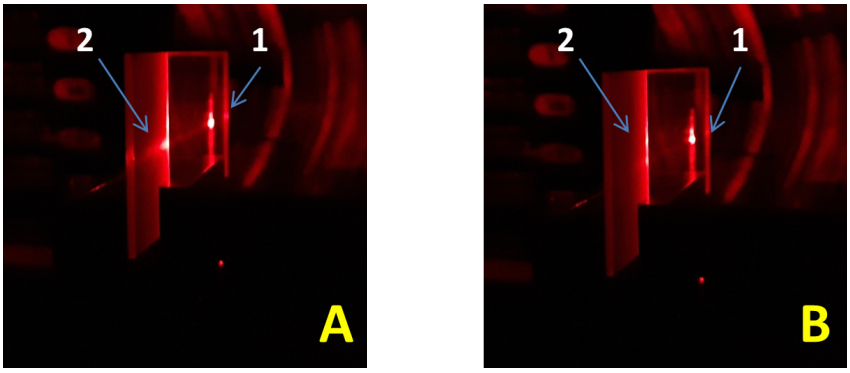

Fig. 9. The optical signal coupling to the grating coupler structure via PMMA Fresnel microlens with an optimum incidence angle (**a**) and non-optimum incidence angle (**b**).

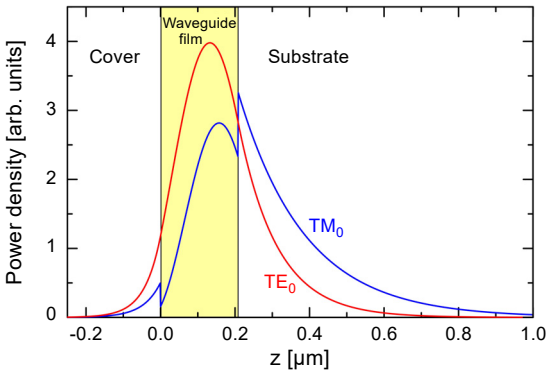

Fig. 10. Power density distribution for the investigated TiO_2-SiO_2 slab waveguide structure.

although very efficient in light coupling are less useful for sensing applications. Extreme cases of such devices are fully etched grating couplers, *e.g.* developed in Si_3N_4 [14] and SOI [15] PIC technologies.

The grating couplers discussed in this paper were developed in order to meet the opposite requirements (*i.e.* highest possible sensitivity). Therefore the small coupling efficiency does not constitute significant problem for the prospective application of the proposed system for sensing, as the detection will be based rather on the optimal incidence angle shift measurement than on absolute measurement of decoupled power. Regardless the low coupling efficiency, the guided mode streak was easily observable at the optimal incidence angle and quickly disappearing with small detuning of an incidence angle from the optimal one.

The operation of sensor structures basing on TiO_2-SiO_2 grating couplers was discussed in depth in Ref. [11]. It was shown that the detection limit for ambient refractive index sensing for the grating coupler having $\chi = 2400$ g/mm was as low as 5.0×10^{-6} RIU.

The presented measurement results were obtained with a TM input polarization state as for this polarization, guided mode streaks were better visible. This was caused by smaller optical signal loss for this polarization than for TE one. The main source of the optical loss for this type of waveguides is scattering on waveguide layer roughness. As it can be seen, in the power density distribution for the investigated waveguide structure (shown in Fig. 10) the power density for the TE polarization is almost 1.5 times higher than for the TM polarization, causing considerable propagation loss.

6. Conclusions and perspectives

In this paper, the possibility of using polymer microlenses for optical signal coupling to the TiO_2-SiO_2 surface grating couplers has been proven for both plano-convex and Fresnel lens design. The proposed optical coupling scheme may find application in readout instruments for low-cost multichannel biochemical sensors.

The obtained results are encouraging and suggest continuation of this research including following developments: (i) design and fabrication of lenses of larger diameter

(up to 2 mm) for obtaining an improved quasi-parallel beam shape, (ii) assembling a fabricated lens array with a multitude of SMFs in a V-groove in order to provide simultaneous optical coupling to several spots on the surface grating coupler and (iii) improving sensor chip quality in order to increase grating uniformity, reduce optical signal diffusion into the glass substrate and to provide easier optical signal decoupling from the guided mode via a chip facet.

Acknowledgements – This work was partially supported by the Polish National Science Centre in the framework of programs Miniatura I decision number 2017/01/X/ST7/01314 and Opus UMO-2017/25/B/ST7/02232.

References

[1] HEIDEMAN R., HOEKMAN M., SCHREUDER E., *TriPleX-based integrated optical ring resonators for lab-on-a-chip and environmental detection*, IEEE Journal of Selected Topics in Quantum Electronics **18**(5), 2012, pp. 1583–1596, DOI: 10.1109/JSTQE.2012.2188382.

[2] ESTEVEZ M.-C., ALVAREZ M., LECHUGA L.M., *Integrated optical devices for lab-on-a-chip biosensing applications*, Laser & Photonics Reviews **6**(4), 2012, pp. 463–487, DOI: 10.1002/lpor.201100025.

[3] CHOCARRO-RUIZ B., HERRANZ S., FERNÁNDEZ GAVELA A., SANCHÍS J., FARRÉ M., PILAR MARCO M., LECHUGA L.M., *Interferometric nanoimmunosensor for label-free and real-time monitoring of Irgarol 1051 in seawater*, Biosensors and Bioelectronics **117**(5), 2018, pp. 47–52, DOI: 10.1016/j.bios.2018.05.044.

[4] KOZMA P., KEHL F., EHRENTREICH-FÖRSTER E., STAMM C., BIER F.F., *Integrated planar optical waveguide interferometer biosensors: a comparative review*, Biosensors and Bioelectronics **58**, 2014, pp. 287–307, DOI: 10.1016/j.bios.2014.02.049.

[5] CLAES T., GIRONES MOLERA J., DE VOS K., SCHACHT E., BAETS R., BIENSTMAN P., *Label-free biosensing with a slot-waveguide-based ring resonator in silicon on insulator*, IEEE Photonics Journal **1**(3), 2009, pp. 197–204, DOI: 10.1109/JPHOT.2009.2031596.

[6] WANGÜEMERT-PÉREZ J.G., HADIJ-ELHOUATI A., SÁNCHEZ-POSTIGO A., LEUERMANN J., XU D., CHEBEN P., ORTEGA-MOÑUX A., HALIR R., MOLINA-FERNÁNDEZ Í., *Subwavelength structures for silicon photonics biosensing*, Optics & Laser Technology **109**, 2019, pp. 437–448, DOI: 10.1016/j.optlastec.2018.07.071.

[7] CARLBORG C.F., GYLFASON K.B., KAŹMIERCZAK A., DORTU F., BAÑULS POLO M.J., MAQUIEIRA CATALA A., KRESBACH G.M., SOHLSTROM H., MOH T., VIVIEN L., POPPLEWELL J., RONAN G., BARRIOS C.A., STEMME G., VAN DER WIJNGAART W., *A packaged optical slot-waveguide ring resonator sensor array for multiplex label-free assays in labs-on-chips*, Lab on a Chip **10**(3), 2010, pp. 281–290, DOI: 10.1039/B914183A.

[8] SCHMITT K., OEHSE K., SULZ G., HOFFMANN CH., *Evanescent field sensors based on tantalum pentoxide waveguides – a review*, Sensors **8**(2), 2008, pp. 711–738, DOI: 10.3390/s8020711.

[9] LUKOSZ W., *Integrated optical chemical and direct biochemical sensors*, Sensors and Actuators B: Chemical **29**(1–3), 1995, pp. 37–50, DOI: 10.1016/0925-4005(95)01661-9.

[10] TIEFENTHALER K., LUKOSZ W., *Sensitivity of grating couplers as integrated-optical chemical sensors*, Journal of the Optical Society of America B **6**(2), 1989, pp. 209–220, DOI: 10.1364/JOSAB.6.000209.

[11] KARASIŃSKI P., *Embossable grating couplers for planar evanescent wave sensors*, Opto-Electronics Review **19**(1), 2011, pp. 10–21, DOI: 10.2478/s11772-010-0056-1.

[12] MANCUSO M., GODDARD J., ERICKSON D., *Nanoporous polymer ring resonators for biosensing*, Optics Express **20**(1), 2012, pp. 245–255, DOI: 10.1364/OE.20.000245.

[13] KAŹMIERCZAK A., DORTU F., SCHREVENS O., GIANNONE D., VIVIEN L., MARRIS-MORINI D., BOUVILLE D., CASSAN E., GYLFASON K.B., SOHLSTRÖM H., SANCHEZ B., GRIOL A., HILL D., *Light coupling and distribution or Si_3N_4/SiO_2 integrated multichannel single-mode sensing system*, Optical Engineering **48**(1), 2009, article 014401, DOI: 10.1117/1.3067875.

[14] Maire G., Vivien L., Sattler G., Kaźmierczak A., Sanchez B., Gylfason K.B., Griol A., Marris-Morini D., Cassan E., Giannone D., Sohlström H., Hill D., *High efficiency silicon nitride surface grating couplers*, Optics Express **16**(1), 2008, pp. 328–333, DOI: 10.1364/OE.16.000328.

[15] Vermeulen D., Selvaraja S., Verheyen P., Lepage G., Bogaerts W., Absil P., Van Thourhout D., Roelkens G., *High-efficiency fiber-to-chip grating couplers realized using an advanced CMOS-compatible Silicon-On-Insulator platform*, Optics Express **18**(17), 2010, pp. 18278–18283, DOI: 10.1364/OE.18.018278.

Received July 20, 2019
in revised form September 30, 2019